

Is T2* Enough to Assess Oxygenation? Quantitative Blood Oxygen Level–Dependent Analysis in Brain Tumor¹

Thomas Christen, PhD
Benjamin Lemasson, PhD
Nicolas Pannetier, PhD
Regine Farion
Chantal Remy, PhD
Greg Zaharchuk, MD, PhD
Emmanuel L. Barbier, PhD

Purpose:

To analyze the contribution of the transverse relaxation parameter (T2), macroscopic field inhomogeneities (ΔB_0), and blood volume fraction (BVF) to blood oxygen level–dependent (BOLD)-based magnetic resonance (MR) measurements of blood oxygen saturation (SO_2) obtained in a brain tumor model.

Materials and Methods:

This study was approved by the local committee for animal care and use. Experiments were performed in accordance with permit 380820 from the French Ministry of Agriculture. The 9L gliosarcoma cells were implanted in the brain of eight rats. Fifteen days later, 4.7-T MR examinations were performed to estimate T2*, T2, BVf, and T2* $\Delta B_{0\text{corrected}}$ in the tumor and contralateral regions. MR estimates of SO_2 were derived by combining T2, BVf, and T2* $\Delta B_{0\text{corrected}}$ according to a recently described quantitative BOLD approach. Scatterplots and linear regression analysis were used to identify correlation between parameters. Paired Student *t* tests were used to compare the tumor region with the contralateral region.

Results:

No significant correlations were found between T2* and any parameter in either tumor tissue or healthy tissue. T2* in the tumor and T2* in the uninvolved contralateral brain were the same (36 msec \pm 4 [standard deviation] vs 36 msec \pm 5, respectively), which might suggest similar oxygenation. Adding T2 information (98 msec \pm 7 vs 68 msec \pm 2, respectively) alone yields results that suggest apparent hypo-oxygenation of the tumor, while incorporating BVf (5.3% \pm 0.6 vs 2.6% \pm 0.3, respectively) alone yields results that suggest apparent hyperoxygenation. MR estimates of SO_2 obtained with a complete quantitative BOLD analysis, although not correlated with T2* values, suggest normal oxygenation (68% \pm 3 vs 65% \pm 4, respectively). MR estimates of SO_2 obtained in the contralateral tissue agree with previously reported values.

Conclusion:

Additional measurements, such as BVf, T2, and ΔB_0 , are needed to obtain reliable information on oxygenation with BOLD MR imaging. The proposed quantitative BOLD approach, which includes these measurements, appears to be a promising tool with which to map tumor oxygenation.

©RSNA, 2011

¹From Inserm, U836-GIN, Équipe 5, Grenoble, France (T.C., B.L., N.P., R.F., C.R., E.L.B.); Department of Radiology, Lucas Center for Imaging, Stanford University, 1201 Welch Rd, MC 5488, Stanford, CA 94305-5488 (T.C., G.Z.); and Oncodesign Biotechnology, Dijon, France (B.L.). Received March 11, 2011; revision requested May 4; revision received July 14; accepted August 11; final version accepted September 1. Address correspondence to T.C. (e-mail: christenthomas@yahoo.fr).

The availability of a technique with which to image brain hypoxia *in vivo* is of considerable interest. Such tools may improve monitoring and optimization of cancer therapies or detection of tumor recurrence (1,2).

Magnetic resonance (MR) imaging is already considered the method of choice in the diagnosis of brain tumors, as it provides information about tumor size and location and extent of edema, as well as hemodynamic information (blood volume fraction [BVf], vessel size index). MR imaging is also sensitive to blood oxygenation via the blood oxygen level–dependent (BOLD) effect (3). Changes in magnetic susceptibility of hemoglobin as it releases oxygen induce perturbations of the magnetic field inside and outside the vessels, decreasing the $T2^*$ relaxation time in an imaging voxel. Thus, $T2^*$ is related to the total amount of deoxyhemoglobin in the voxel and, by extension, the blood oxygen saturation (SO_2) and partial pressure of oxygen in and around blood vessels. In the healthy brain, BOLD imaging is sensitive to variations in the inspired oxygen fraction (4) and is related to the SO_2 of major arteries and veins (5). The appeal of mapping blood SO_2 with BOLD MR imaging relies on its noninvasiveness and widespread availability in clinical imagers. It could provide good spatial and temporal

resolution and could be coregistered with anatomic and functional information on the tumor microenvironment.

Because of these features, recent studies have proposed the use of $T2^*$ estimates to assess tumor oxygenation (6–8). However, it is important to realize that the $T2^*$ of a particular voxel is not purely a reflection of blood SO_2 but that it also depends on other parameters. Microscopic nuclear electron interactions between neighbor atoms give rise to a dissipative relaxation mechanism described by $T2$. This transverse relaxation time may be linked to $T2^*$ by using the following equation: $1/T2^* = 1/T2 + 1/T2'$. Macroscopic field inhomogeneities, which may originate from magnet imperfections, poor shimming, tissue-air interfaces, or other causes, may affect the measurement and level of tissue oxygenation. $T2^*$ is sensitive to the total amount of deoxyhemoglobin in the voxel. Thus, knowledge of BVf is of tantamount importance. Particularly, tumor BVf varies in space and time as the tumor grows and matures (9,10).

Recently, it has been shown that these other factors can be combined according to a mathematic model to obtain quantitative MR estimates of SO_2 (11). This quantitative BOLD approach, which follows the work pioneered by An and Lin (12) and which was refined by He and Yablonskiy (13), has shown encouraging results in the healthy rat brain (11). However, it remains unclear whether the additional factors included in the quantitative BOLD calculations are really necessary to accurately measure SO_2 in the brain. Is one $T2^*$ measurement sufficient to determine the tumor oxygenation level? In this study, we analyzed the contribution of the transverse relaxation parameter ($T2$), macroscopic field inhomogeneities, and BVf to BOLD-based MR estimates of SO_2 obtained in a brain tumor model.

Materials and Methods

No industry support was received for this study; costs were covered by intramural Institut National de la Sante et de la Recherche Medicale funding. One author (E.L.B.) contacted Guerbet

(Aulnay-sous-Bois, France) to obtain the contrast agent. One author (B.L.) is an employee of Oncodesign Biotechnology. The other authors, none of whom has a reportable relationship with industry, collectively had control over the inclusion of any data and information that might have presented a conflict of interest for this author. The study design was approved by the local committee for animal care and use. Experiments were performed in accordance with permit 380820 from the French Ministry of Agriculture.



Animals and Tumor Model

An author (B.L., 4 years of experience in tumor models) implanted 9L gliosarcoma cells (14) in the brain of eight male Fischer (Charles River, L'Abresle, France) rats (weight range, 120–150 g), as described previously (15). Briefly, tumor cell inoculation was performed after the rats had been anesthetized. Anesthesia was achieved by using 5% isoflurane for induction and intraperitoneal injection of ketamine (64.5 mg per kilogram of body weight, Ketamine 500; Centravet, Lapalisse, France) and xylazine (5.4 mg/kg, Rompun; Centravet) in saline. An inoculation of 1 μ L

Advances in Knowledge

- Additional MR measurements, such as the transverse relaxation parameter, macroscopic field inhomogeneities, and blood volume fraction, are necessary to make an accurate assessment of tissue oxygenation with blood oxygen level–dependent (BOLD) MR imaging; failure to include any of these parameters may lead to incorrect conclusions about tumor oxygenation.
- The proposed quantitative BOLD approach, which includes the aforementioned measurements, appears to be a promising tool with which to map blood oxygen saturation.

Published online before print

10.1148/radiol.11110518 Content codes:  

Radiology 2012; 262:495–502

Abbreviations:

BOLD = blood oxygen level–dependent
 BVf = blood volume fraction
 ROI = region of interest
 SO_2 = blood oxygen saturation

Author contributions:

Guarantors of integrity of entire study, T.C., B.L., C.R., E.L.B.; study concepts/study design or data acquisition or data analysis/interpretation, all authors; manuscript drafting or manuscript revision for important intellectual content, all authors; manuscript final version approval, all authors; literature research, T.C., N.P., G.Z., E.L.B.; experimental studies, T.C., B.L., R.F., C.R., G.Z., E.L.B.; statistical analysis, T.C., B.L.; and manuscript editing, T.C., B.L., N.P., C.R., G.Z., E.L.B.

Funding:

This research was supported by the National Institutes of Health (grants R01NS066506 and R01 NS047607).

Potential conflicts of interest are listed at the end of this article.

See also Science to Practice in this issue.

of cell suspension in serum-free Roswell Park Memorial Institute 1640 medium (Invitrogen, Pontoise, France) containing 10^4 cells was administered in the right caudate nucleus through a 1-mm burr hole 3.5 mm lateral from the bregma. After injection, the burr hole was filled, the skin incision was sewn shut, and animals were revived in an incubator before they were returned to the animal facility (15).

MR Imaging

Fifteen days after inoculation, MR imaging was performed at 4.7 T (Avance III console; Bruker, Wissembourg, France) by using volume and surface cross coil configuration (T.C., B.L.; each with 4 years of experience in MR imaging). Animals were given 5% isoflurane in air for induction of anesthesia and 2% isoflurane in air for maintenance of anesthesia. A catheter was inserted in the tail vein to deliver the contrast agent. Animals were held in place in the MR imager with a head holder and teeth bars. Animals were breathing freely in a facemask, and rectal temperature was maintained at 37.0°C via a heating blanket. After careful shimming, the following MR sequences were performed in the axial plane.

Anatomic sequence.—T2-weighted images were acquired with a spin-echo MR sequence and the following parameters: repetition time msec/echo time msec, 4000/33; two signals acquired; 19 sections with 30 × 30-mm field of view; matrix, 256 × 256; voxel size, 117 × 117 × 1000 μm. Acquisition duration was 4 minutes 17 seconds.

Multiple spin-echo sequence.—A multiple spin-echo two-dimensional sequence was performed with the following parameters: 1500/15; 20 spin echoes; change in echo time, 12 msec; field of view, 30 × 30 mm; matrix, 128 × 128; voxel size, 234 × 234 × 1000 μm. Acquisition duration was 3 minutes 40 seconds.

Multiple gradient-echo three-dimensional sequence.—A multiple gradient-echo three-dimensional sequence was performed with the following parameters: 100/4; 15 gradient echoes; change in echo time, 4 msec; field of

view, 30 × 30 × 4 mm; matrix, 256 × 256 × 20; voxel size, 117 × 117 × 200 μm. Acquisition duration was 12 minutes 48 seconds.

Multiple gradient-echo and spin-echo sequence.—A multiple gradient-echo and spin-echo sequence was performed with the following parameters: 6000/3; eight gradient echoes; change in echo time, 3 msec; duration of one spin echo, 60 msec; field of view, 30 × 30 mm; matrix, 128 × 128; voxel size, 234 × 234 × 1000 μm. Acquisition duration was 6 minutes. This sequence was performed before and after administration of ultrasmall superparamagnetic iron oxide via the tail vein (200 μmol of iron per kilogram of body weight) (Sinerem, Guerbet, Roissy, France; Combidex, AMAG Pharmaceuticals, Lexington, Mass).

MR Data Analysis

Processing was performed within the Matlab 7 environment (MathWorks, Natick, Mass) by using custom software, as will be described (T.C., B.L., N.P., E.L.B., C.R.; 4, 4, 4, 15, and 20 years of experience in MR imaging, respectively).

Transverse relaxation times.— $T2^*$ was calculated by using a nonlinear exponential fit (preferred to a linear fit after log transformation [16]) of the gradient-echo signal of the multiple gradient-echo and spin-echo sequence. To avoid the initial nonexponential phase of MR signal decay, the initial 10 msec of signal decay were not included during fitting (11). To remove macroscopic inhomogeneities from the voxel $T2^*$, which was termed $T2^* \Delta_{B0corrected}$, the multiple gradient-echo three-dimensional sequence was used. Each of the thin sections (200 μm thick) was averaged to form the same 1000-μm section thickness as that used for $T2^*$ measurements. An exponential fit of this signal evolution yielded corrected $T2^* \Delta_{B0corrected}$. $T2$ was computed by fitting a nonlinear exponential fit of the multiple spin-echo data. Finally, $T2'$ (a relaxation parameter equal to $T2^*$ corrected for spin-spin effects) was computed as $1/(1/T2^* - 1/T2)$, and $T2' \Delta_{B0corrected}$ was calculated as $1/(1/T2^* \Delta_{B0corrected} - 1/T2)$.

BVf estimation.—BVf was estimated by using the steady-state approach described by Tropres et al (17) and according to the formula:

$$BVf = \frac{3}{4 \cdot \pi \cdot \gamma \cdot \Delta\chi_{USPIO} \cdot B_0} \cdot \left(\frac{1}{T2^*_{after}} - \frac{1}{T2^*_{before}} \right), \quad (1)$$

where $T2^*_{before}$ and $T2^*_{after}$ correspond to the transverse relaxation time obtained before and after injection of the contrast agent, respectively. The change of susceptibility after injection of the contrast agent (ultrasmall superparamagnetic iron oxide) is represented by $\Delta\chi_{USPIO}$ and is equal to 0.231 ppm (centimeter-gram-second unit) (18). The proton gyromagnetic ratio is represented by γ and is equal to 2.67502×10^8 rad/s/T.

Tissue SO_2 .—MR estimation of SO_2 (MR- SO_2) was performed by using a previously described quantitative BOLD approach (11). This technique uses a mathematic model of MR signal time evolution in a gradient-echo experiment and a combination of MR-derived parameters. The following equation was fitted to the MR signal decay, represented by $s(t)$, beyond 10 msec of the volume-averaged multiple gradient-echo three-dimensional sequence:

$$s(t) = Cte \cdot \exp\left[-\frac{1}{T2} \cdot t - BVf \cdot \gamma \cdot \frac{4}{3} \cdot \pi \cdot \Delta\chi_0 \cdot Hct \cdot (1 - MR_{SO2}) \cdot B_0 \cdot t\right], \quad (2)$$

by using $T2$ and BVf from the corresponding maps. The microvascular hematocrit fraction (Hct) was set to 0.42 · 0.85 (85% of the macrovascular hematocrit level) (11). The difference between the magnetic susceptibilities (expressed in centimeter-gram-second) of fully oxygenated and fully deoxygenated hemoglobin ($\Delta\chi_0$) was set to 0.264 ppm (19). Cte is a proportionality constant that depends on different parameters—such as spin density, flip angle, magnetic field, and hardware sensitivity—and B_0 is equal to 4.7 T.

Tumor regions of interest (ROIs) were manually delineated on the anatomic

Table 1

MR-derived Measurements in Contralateral and Tumor ROIs

ROI	T2* (msec)	T2 (msec)	T2' (msec)	T2* Δ B _{0corrected} (msec)	T2' Δ B _{0corrected} (msec)	BVf (%)	MR Estimate of SO ₂ (%)
Contralateral	36 ± 5	68 ± 2	99 ± 39	51 ± 1	383 ± 204	2.6 ± 0.3	65 ± 4
Tumor	36 ± 4	98 ± 7	69 ± 16	56 ± 5	185 ± 30	5.3 ± 0.6	68 ± 3

Note.—Data are means ± standard deviations.

Figure 1

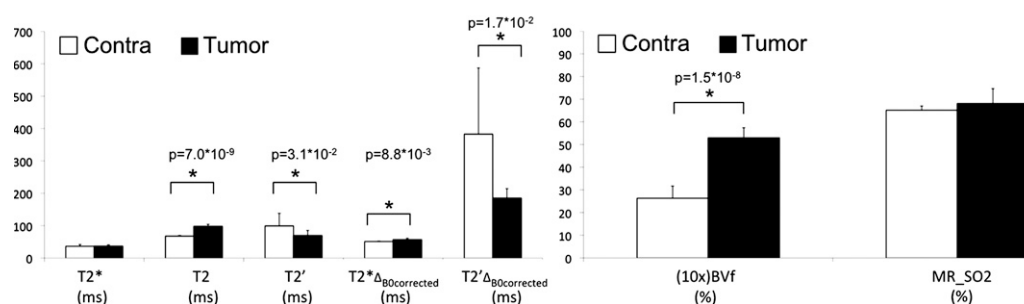


Figure 1: Graphs show MR parameters obtained in tumor and contralateral regions in eight rats. Data are mean ± standard deviation. MR_SO₂ = MR estimate of SO₂. * = $P < .05$.

T2-weighted images (B.L., 4 years of experience with tumor models). ROIs were also drawn in the contralateral striatum on the same sections (considered healthy tissue). The mean ROI size across animals was 140 mm³ ± 98 (standard deviation). Each ROI was transferred on T2*, T2* Δ B_{0corrected}, T2, T2', T2' Δ B_{0corrected}, BVf, and final calculated MR estimates of SO₂ maps. Some voxels were then excluded from the ROI. Exclusion criteria were as follows: voxel for which fitting did not converge, voxel with negative BVf or MR estimates of SO₂ (corresponding to nonphysiologic values), voxels with MR estimates of SO₂ above 100% (corresponding to nonphysiologic values), and voxels with BVf values outside the range of validity of the method (BVf > 17%) (20). Less than 10% of the pixels were excluded according to these criteria.

Statistical Analysis

Paired Student *t* tests were used to compare the tumoral region with the contralateral region. Values were considered significantly different when the *P* value was less than .05. The Pearson correlation coefficient was computed to

determine if BVf, T2* Δ B_{0corrected}, T2, or MR estimates of SO₂ were predictors of T2*. Log transformation of the outcome was considered to increase the accuracy of the linear regression procedure.

Results

We present in Table 1 and Figure 1 the quantitative results obtained for all MR-derived parameters. Mean and standard deviation for the eight rats are given for the tumor and contralateral ROIs. A T2* value of about 36 msec was found in both ROIs. However, T2 in the tumor ROI was 30 msec longer than that in the contralateral ROI. Accordingly, the derived T2' is lower in the tumor than in the contralateral ROI. The correction for macroscopic inhomogeneities substantially increases the T2* value in both ROIs. Tumor T2* Δ B_{0corrected} is longer than that of contralateral tissue. Thus, T2' Δ B_{0corrected}, which reflects both T2* Δ B_{0corrected} and T2 differences between regions, is significantly lower in the tumor ROI than in the contralateral ROI. Conversely, the tumor BVf is significantly higher than that in the contralateral ROI (5.3% vs 2.6%, $P <$

.0001). Use of the quantitative BOLD approach to combine these estimates leads to an MR estimate of SO₂ of 65% ± 4 in the contralateral ROI. At this growth stage, the MR estimate of SO₂ in the 9L gliosarcoma cell tumor is comparable with that in contralateral tissue (68% ± 3 vs 65% ± 4, $P = .12$).

Figure 2 shows examples of T2, T2*, T2* Δ B_{0corrected}, T2' Δ B_{0corrected}, BVf, and MR estimates of SO₂ maps obtained in one representative animal. The tumor ROI is shown. Visually, it is clear that the T2* Δ B_{0corrected} map is more homogeneous than the original T2* map. The MR estimates of the SO₂ map, although relatively uniform in gray matter, exhibit significantly lower MR estimates of SO₂ values in the corpus callosum.

Scatterplots of the different parameters pitted against one another were obtained to enable us to identify correlations between MR-derived parameters. An example in one animal is shown in Figure 3. The values correspond to voxels inside both tumor and contralateral ROIs. The equation of the regression line and *R*² are given for each graph. No linear correlation was found between the parameters. On the T2* versus T2

Figure 2

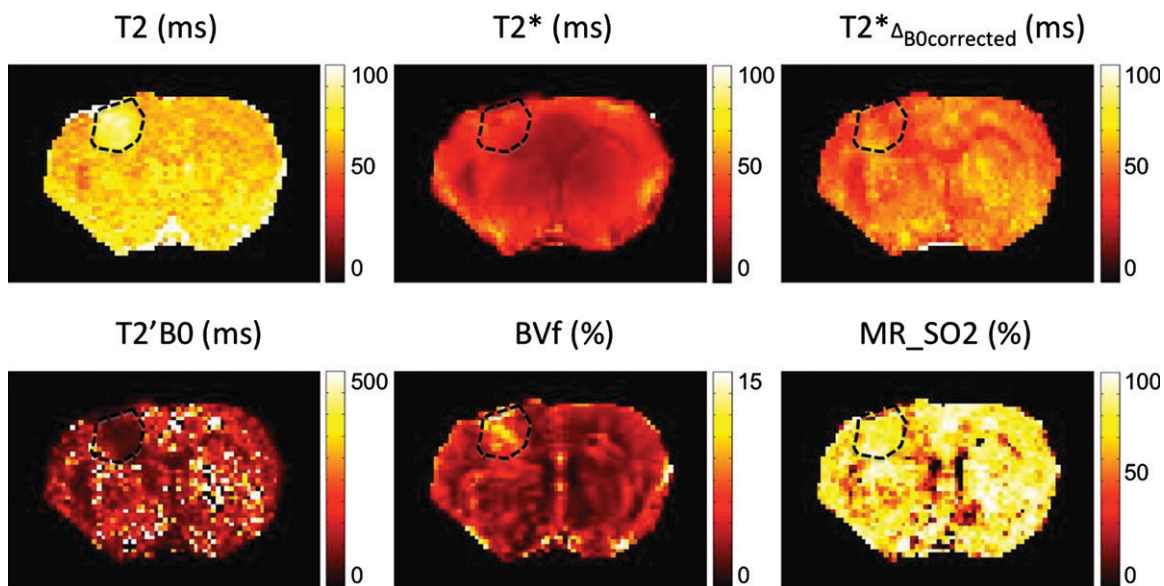


Figure 2: Parametric maps obtained in one representative rat. Dashed lines represent tumor ROI superimposed on anatomic images.

Figure 3

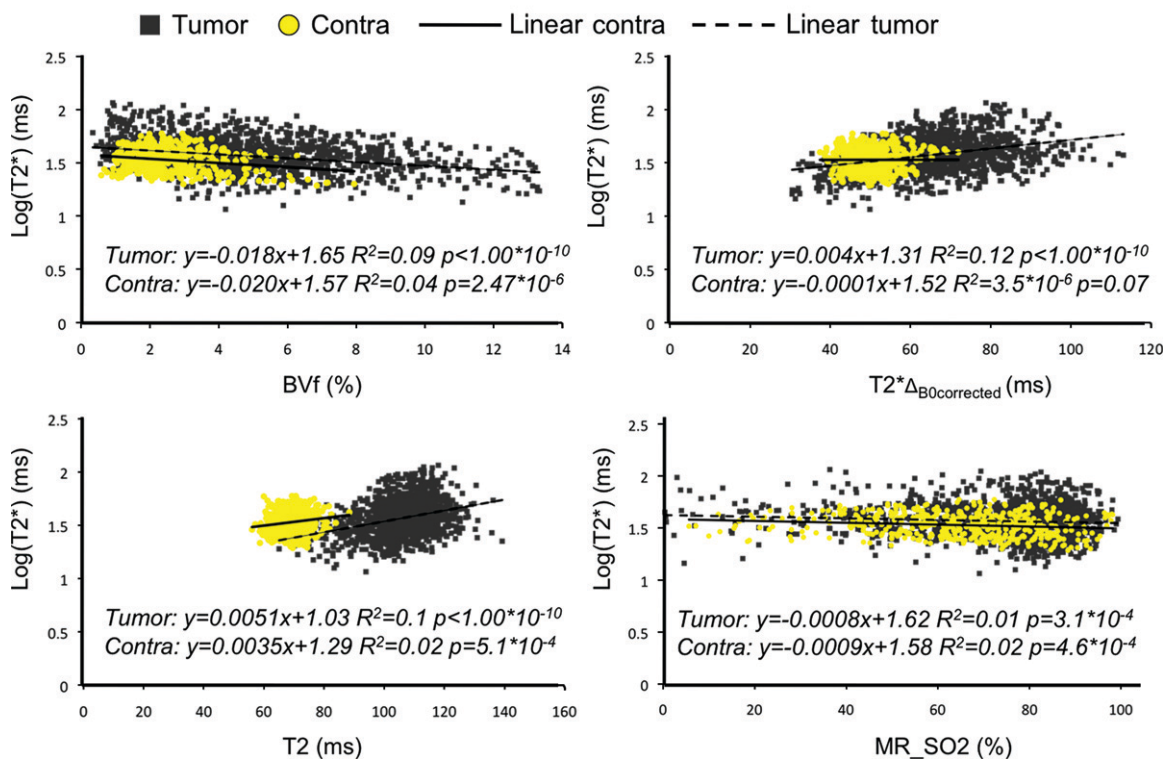


Figure 3: Scatterplots show MR estimates of T2* as a function of BVf, T2*ΔB₀corrected, T2, and MR estimate of SO₂ (MR_SO₂) in tumor and contralateral regions in one rat. Linear regression curves, as well as corresponding equations and correlation coefficients, are given for each scatterplot.

Table 2

Cross-correlation Coefficients between MR Parameters Obtained in All Rats in Contralateral and Tumor ROIs

Rat No.	Contralateral ROI				Tumor ROI					
	T2* vs T2	T2* vs T2* Δ B _{0corrected}	T2* vs BVf	T2* vs MR Estimate of SO ₂	MR Estimate of SO ₂ vs BVf	T2* vs T2	T2* vs T2* Δ B _{0corrected}	T2* vs BVf	T2* vs MR Estimate of SO ₂	MR Estimate of SO ₂ vs BVf
1	0.1823	0.0006	0.0527	0.0474	0.359	0.1831	0.1398	0.153	0.0131	0.555
2	0.0045	0.2341	0.0084	0.0003	0.3091	0.0568	0.1251	0.043	0.0003	0.5052
3	0.0005	0.0526	0.2136	0.0197	0.2283	0.1055	0.135	0.2027	0.1157	0.1157
4	0.0254	0.141	0.042	0.0219	0.4062	0.1013	0.3359	0.0956	0.007	0.4104
5	0.02	0.4894	0.0001	0.0015	0.242	0.0137	0.2023	0.0356	0.0009	0.4246
6	0.0005	0.1858	0.0019	0.0055	0.401	0.0499	0.2182	0.0883	0.0009	0.4019
7	0.0274	0.087	0.0007	0.0111	0.0533	0.0266	0.068	0.0001	0.0131	0.3959
8	0.0482	0.3454	0.022	0.0176	0.1225	0.1106	0.1003	0.089	0.0107	0.3443
Mean \pm standard deviation	0.0386 \pm 0.0603	0.1920 \pm 0.1619	0.0427 \pm 0.0719	0.0156 \pm 0.0152	0.2652 \pm 0.1288	0.0809 \pm 0.0552	0.1656 \pm 0.0846	0.0884 \pm 0.0654	0.0202 \pm 0.0390	0.3941 \pm 0.1306

scatterplot, the tumor and contralateral voxels can be distinguished clearly. This distinction is not noted for the other parameter combinations. Table 2 summarizes the linear regression coefficients obtained for each animal and for each combination of parameters. All R^2 values were less than 0.35, suggesting an absence of linear relation between the estimates. Visual analysis of the scatterplots indicates a larger dispersion of the values in the lesion, in agreement with the heterogeneous nature of the tumor microenvironment. Visual analysis of the plot also suggests that the parameters are not linked with a nonlinear relationship.

MR estimates of SO₂, although derived from a combination of all parameters, do not show correlation with the T2* values. This observation suggests that the two estimates yield different information. We also plotted BVf versus MR estimates of SO₂ for all rats to evaluate the dependence of the two parameters (Fig 4). We found a clear nonlinear relationship between the two estimates. Three regions can be distinguished. First, in the range of normal BVf values (2%–5%), there is poor correlation between BVf and MR estimates of SO₂. Second, in regions with high BVf, only high MR estimates of SO₂ values (about 80%) are found. On the contrary, for small BVf, only small MR estimates of SO₂ values are obtained. These results are in agreement with the concept that the tumor tissue extracts more oxygen from blood as BVf decreases to maintain a constant SO₂ level.

Discussion

It has been proposed that BOLD oximetry could be a sensitive tool with which to characterize the tumor oxygenation level. Despite the positive findings in previous studies (6,7), the T2*-based method may suffer from dependence of the BOLD signal on various parameters. Indeed, T2* depends on the vascular oxygenation level, but it also depends on T2 (sensitive to tissue edema) and BVf (sensitive to angiogenesis), as well as on macroscopic magnetic field inhomogeneities. Thus, a strategy that

includes additional MR measurements, such as BVf (7,21) and T2 (22), is likely to improve both sensitivity and specificity of the T2*-based oximetry. In this study, we measured and characterized the relationship between T2*, T2, macroscopic field inhomogeneities, and BVf in a rat brain tumor model.

Our findings indicate that these parameters are largely independent of each other and vary in the tumor environment. The oxygenation status of the tumor appears to depend on the number of parameters included in analysis of the T2*-based oximetry. While T2* maps suggest a normal oxygenation level in the tumor, introducing a correction for T2 variations or for macroscopic inhomogeneities of B_0 yields a hypoxic tumor. Alternatively, incorporating BVf information alone to the raw T2* data leads to the opposite conclusion (a hyperoxic tumor).

To improve the specificity of BOLD oximetry, we recently proposed a mathematic model that combines all of the additional parameters and yields a quantitative estimate of SO_2 (11). The method differs from the previous quantitative BOLD attempts, as we used independent measurements of T2 and BVf to extract oxygenation information from T2* maps. This approach was motivated by results obtained recently that show that quantitative BOLD results have more uncertainty if all parameters are optimized simultaneously during the nonlinear fitting process (21,23). However, if one or more of the parameters was fixed to an independent predetermined value, MR estimates of SO_2 were estimated correctly (21). Numeric simulations (11) also suggest that incorporating BVf measurements into the model will lead to MR estimates of SO_2 measurements that correspond quantitatively to the SO_2 averaged across the arteriovenous networks within the voxel. We further validated this in the healthy rat brain by comparing MR estimates of SO_2 and blood gas measurements (11). In our study, the MR estimate of SO_2 is about 65% in the contralateral hemisphere. This finding is in agreement with our findings in healthy rats and with values obtained with other

Figure 4

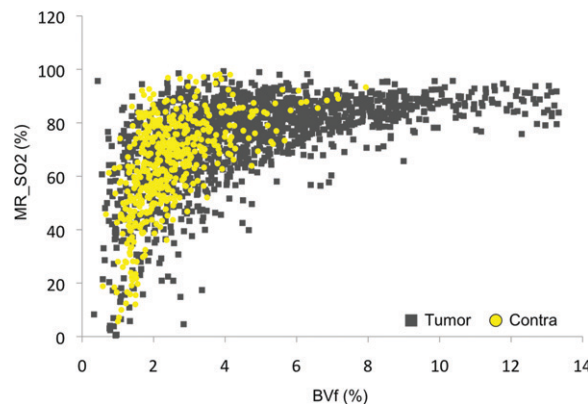


Figure 4: MR estimate of SO_2 (MR_SO_2) as a function of BVf measured in the tumor or contralateral region in one rat.

approaches, such as near-infrared spectroscopy (24). At first blush, the conclusions drawn from the quantitative BOLD approach appear to agree with those drawn from the uncorrected T2* estimates (similar SO_2 in the tumor and healthy tissue). However, it can be seen in Table 1 that the similar T2* values obtained for the two regions arise from cancellation of the competing effects of the increase in the tumor T2 and BVf (particular to this tumor model at this growth stage) rather than being due to a direct effect of the blood oxygenation. Indeed, it is well known that tumors may exhibit various patterns of edema (leading to T2 variations), angiogenesis (leading to BVf variations), or necrosis (leading to T2* being equal to T2 and BVf being equal to 0) (18). Although comparisons with other approaches, such as near-infrared spectroscopy, positron emission tomography, or pimonidazole administration, should be performed to validate the MR estimates of SO_2 measurements in the tumor, the results obtained in our study indicate that the conclusions derived from the quantitative BOLD approach are likely to be more specific to oxygenation than T2* measurements alone.

It is also important to recognize potential limitations to the quantitative BOLD approach described here. First, T2* yields information on SO_2 instead of on the tissue oxygen partial pressure currently used to define tumor hypoxia. Although a relationship between tissue oxygen partial pressure and SO_2 can be derived in the vicinity of blood vessels,

it is not clear that this applies to the tumor environment. Nevertheless, recent studies in which researchers compared BOLD MR imaging and immunohistochemistry suggest a direct relationship between T2* and hypoxia. McPhail and Robinson (25) showed correlation between baseline $R2^*$ (equivalent to $1/T2^*$) and pimonidazole adduct formation in a model of rat mammary tumor. Baseline T2* has also been shown to have high sensitivity in the definition of tumor hypoxia in human prostate tumor (6,7). Second, some assumptions of the mathematic model, such as restricted water diffusion or homogeneous vascular geometry, may induce bias in the MR estimates of SO_2 estimates (23,26). The main source of error in the MR estimation of SO_2 remains the presence of non-vascular magnetic susceptibility sources in the voxel. For example, it is not possible to distinguish the presence of deoxyhemoglobin from the presence of iron by using MR techniques. Thus, in the case of a hemorrhagic tumor, the MR estimation of SO_2 is likely to be biased.

Further improvement of the quantitative BOLD approach is possible. In its current form, the method is applicable in only animals since iron oxide particle-based contrast agents are not yet approved for routine use in patients. Bolus tracking techniques, such as dynamic susceptibility contrast material-enhanced MR imaging, are routinely used in patients and can yield accurate BVf measurements. The combination of ASL and DSC could also help to increase the accuracy of the BVf measurements

and would enable MR estimation of cerebral metabolic rate of O_2 through the addition of the blood flow measurement (27). The acquisition time could also be reduced by using rapid acquisition schemes, such as echo planar or spiral MR imaging, and/or MR sequences that enable direct estimation of $T2'$, such as asymmetric spin-echo (28) or combined gradient-echo and spin-echo approaches (29).

Practical application: Our study results enabled us to confirm recent observations that additional measurements, such as $T2$, $T2^* \Delta_{BOLD\text{corrected}}$, and BVf, are integral to the accurate assessment of tissue oxygenation with BOLD MR imaging and that lack of inclusion of any of these parameters may lead to incorrect conclusions about tumor oxygenation. Although it needs further validation, the proposed quantitative BOLD approach, which combines the previously mentioned parameters, appears to be a promising tool with which to measure SO_2 . Given that it is minimally invasive, this $T2^*$ -based quantitative BOLD approach could be extended to study hypoxia in other tumor models or to improve the ability to describe the ischemic penumbra in patients who have had a stroke.

Disclosures of Potential Conflicts of Interest: **T.C.** No potential conflicts of interest to disclose. **B.L.** Financial activities related to the present article: none to disclose. Financial activities not related to the present article: is an employee of Oncodesign Biotechnology. Other relationships: none to disclose. **N.P.** No potential conflicts of interest to disclose. **R.F.** No potential conflicts of interest to disclose. **C.R.** No potential conflicts of interest to disclose. **G.Z.** Financial activities related to the present article: none to disclose. Financial activities not related to the present article: is a member of the GE Healthcare Neuroradiology Advisory board, institution received funds from GE Healthcare Research Support. Other relationships: none to disclose. **E.L.B.** No potential conflicts of interest to disclose.

References

- Vaupel P, Mayer A. Hypoxia in cancer: significance and impact on clinical outcome. *Cancer Metastasis Rev* 2007;26(2):225–239.
- Tatum JL, Kelloff GJ, Gillies RJ, et al. Hypoxia: importance in tumor biology, non-invasive measurement by imaging, and value of its measurement in the management of cancer therapy. *Int J Radiat Biol* 2006;82(10):699–757.
- Ogawa S, Lee TM, Kay AR, Tank DW. Brain magnetic resonance imaging with contrast dependent on blood oxygenation. *Proc Natl Acad Sci U S A* 1990;87(24):9868–9872.
- Lu J, Dai G, Egi Y, et al. Characterization of cerebrovascular responses to hyperoxia and hypercapnia using MRI in rat. *Neuroimage* 2009;45(4):1126–1134.
- Lin W, Paczynski RP, Celik A, Kuppasamy K, Hsu CY, Powers WJ. Experimental hypoxic hypoxia: changes in $R2^*$ of brain parenchyma accurately reflect the combined effects of changes in arterial and cerebral venous oxygen saturation. *Magn Reson Med* 1998;39(3):474–481.
- Chopra S, Foltz WD, Milosevic MF, et al. Comparing oxygen-sensitive MRI (BOLD $R2^*$) with oxygen electrode measurements: a pilot study in men with prostate cancer. *Int J Radiat Biol* 2009;85(9):805–813.
- Hoskin PJ, Carnell DM, Taylor NJ, et al. Hypoxia in prostate cancer: correlation of BOLD-MRI with pimonidazole immunohistochemistry—initial observations. *Int J Radiat Oncol Biol Phys* 2007;68(4):1065–1071.
- Rodrigues LM, Howe FA, Griffiths JR, Robinson SP. Tumor $R2^*$ is a prognostic indicator of acute radiotherapeutic response in rodent tumors. *J Magn Reson Imaging* 2004;19(4):482–488.
- Avni R, Cohen B, Neeman M. Hypoxic stress and cancer: imaging the axis of evil in tumor metastasis. *NMR Biomed* 2011;24(6):569–581.
- Padhani A. Science to practice: what does MR oxygenation imaging tell us about human breast cancer hypoxia? *Radiology* 2010;254(1):1–3.
- Christen T, Lemasson B, Pannetier N, et al. Evaluation of a quantitative blood oxygenation level-dependent (qBOLD) approach to map local blood oxygen saturation. *NMR Biomed* 2010;24(4):393–403.
- An H, Lin W. Quantitative measurements of cerebral blood oxygen saturation using magnetic resonance imaging. *J Cereb Blood Flow Metab* 2000;20(8):1225–1236.
- He X, Yablonskiy DA. Quantitative BOLD: mapping of human cerebral deoxygenated blood volume and oxygen extraction fraction—default state. *Magn Reson Med* 2007;57(1):115–126.
- Benda P, Someda K, Messer J, Sweet WH. Morphological and immunochemical studies of rat glial tumors and clonal strains propagated in culture. *J Neurosurg* 1971;34(3):310–323.
- Bräuer-Krisch E, Requardt H, Brochard T, et al. New technology enables high precision multislit collimators for microbeam radiation therapy. *Rev Sci Instrum* 2009;80(7):074301.
- Xing L, Hornak JP. $T2$ calculations in MRI: linear versus nonlinear methods. *J Imaging Sci Technol* 1994;38(2):154–157.
- Tropès I, Lamalle L, Péoc'h M, et al. In vivo assessment of tumoral angiogenesis. *Magn Reson Med* 2004;51(3):533–541.
- Valable S, Lemasson B, Farion R, et al. Assessment of blood volume, vessel size, and the expression of angiogenic factors in two rat glioma models: a longitudinal in vivo and ex vivo study. *NMR Biomed* 2008;21(10):1043–1056.
- Spees WM, Yablonskiy DA, Oswood MC, Ackerman JJ. Water proton MR properties of human blood at 1.5 Tesla: magnetic susceptibility, $T(1)$, $T(2)$, $T^*(2)$, and non-Lorentzian signal behavior. *Magn Reson Med* 2001;45(4):533–542.
- Tropès I, Grimault S, Vaeth A, et al. Vessel size imaging. *Magn Reson Med* 2001;45(3):397–408.
- Sedlacik J, Reichenbach JR. Validation of quantitative estimation of tissue oxygen extraction fraction and deoxygenated blood volume fraction in phantom and in vivo experiments by using MRI. *Magn Reson Med* 2010;63(4):910–921.
- Saitta L, Heese O, Förster AF, et al. Signal intensity in $T2'$ magnetic resonance imaging is related to brain glioma grade. *Eur Radiol* 2011;21(5):1068–1076.
- Sohlin MC, Schad LR. Susceptibility-related MR signal dephasing under nonstatic conditions: experimental verification and consequences for qBOLD measurements. *J Magn Reson Imaging* 2011;33(2):417–425.
- Sakata YS, Grinberg OY, Grinberg S, Springett R, Swartz HM. Simultaneous NIR-EPR spectroscopy of rat brain oxygenation. *Adv Exp Med Biol* 2005;566:357–362.
- McPhail LD, Robinson SP. Intrinsic susceptibility MR imaging of chemically induced rat mammary tumors: relationship to histologic assessment of hypoxia and fibrosis. *Radiology* 2010;254(1):110–118.
- Dickson JD, Ash TWJ, Williams GB, et al. Quantitative BOLD: the effect of diffusion. *J Magn Reson Imaging* 2010;32(4):953–961.
- Zaharchuk G, Straka M, Marks MP, Albers GW, Moseley ME, Bammer R. Combined arterial spin label and dynamic susceptibility contrast measurement of cerebral blood flow. *Magn Reson Med* 2010;63(6):1548–1556.
- An H, Lin W. Impact of intravascular signal on quantitative measures of cerebral oxygen extraction and blood volume under normo- and hypercapnic conditions using an asymmetric spin echo approach. *Magn Reson Med* 2003;50(4):708–716.
- Fujita N, Shinohara M, Tanaka H, Yutani K, Nakamura H, Murase K. Quantitative mapping of cerebral deoxyhemoglobin content using MR imaging. *Neuroimage* 2003;20(4):2071–2083.